RAS Family Gene Mutations, Clinicopathological Features, and Spread Patterns of Inverted Urothelial Papilloma of the Bladder

Keiichiro Kitahama, MD,†‡ Yasuyuki Shigematsu, MD, PhD,*† Gulanbar Amori, MD, PhD,*† Emiko Sugawara, MD, PhD,*† Junji Yonese, MD, PhD,§ Junji Shibahara, MD, PhD,‡ Kengo Takeuchi, MD, PhD,*†‖ and Kentaro Inamura, MD, PhD*†*

Abstract: Inverted urothelial papilloma (IUP) is a benign neoplasm characterized by a downgrowth of the urothelium beneath the surface of morphologically normal urothelial cells; however, the molecular features of IUP and their association with clinicopathological characteristics are unclear. In this study, we aimed to investigate the mutational landscape, clinicopathological features, genotype-phenotype associations, and spread patterns of IUP. We performed targeted next-generation sequencing of 39 consecutive IUP cases, the largest series investigated to date, and identified oncogenic driver mutations in RAS family genes in 34 cases (87%). *HRAS* mutations were the most prevalent (28 cases), which included Q61R (15 cases), followed by *KRAS* (5 cases) and *NRAS* (1 case) mutations. Characteristic mutations observed in urothelial carcinoma, including those in *FGFR3*, *TP53*, or the *TERT* promoter, were absent. *HRAS*-mutated IUPs were associated with a history of smoking ($P = 0.017$) and streaming morphology ($P < 0.001$), corresponding to the trabecular subtype. In contrast, all *KRAS*-mutated IUPs occurred in never-smoking patients ($P = 0.001$) and showed cystic changes in morphology ($P = 0.005$), corresponding to the glandular subtype. RAS Q61R immunohistochemistry visually revealed the neoplastic nature of the overlying cells and distinct spread patterns of IUP cells within the surface, including pseudoinfiltrative spread. No recurrence or carcinoma development was observed in any of the IUP cases during the follow-up period. Thus, we confirmed the importance of RAS pathway activation in IUP pathogenesis, an association between RAS family gene mutations and IUP subtypes, and the spread patterns of IUP cells within the surface.

Key Words: bladder tumor, inverted urothelial papilloma, morphology, RAS pathway

(*Am J Surg Pathol* 2023;00:000–000)

From the *Division of Pathology, The Cancer Institute; †Department of Pathology, The Cancer Institute Hospital; §Department of Genitourinary Oncology, The Cancer Institute Hospital; ‖Pathology Project for Molecular Targets, The Cancer Institute, Japanese Foundation for Cancer Research; and ‡Department of Pathology, Kyorin University School of Medicine, Tokyo, Japan.

K.K., J.S., and K.I.: conceived and designed the study. K.K., Y.S., G.A., E.S., J.Y., K.T., and K.I.: contributed to the acquisition of clinical and tumor tissue data. K.K. and Y.S.: performed data analyses. K.K., Y.S., and K.I.: interpretation of the findings. K.K. and K.I.: drafted the manuscript.

This study was conducted in accordance with the guidelines of the Declaration of Helsinki and approved by the Institutional Review Board of the Japanese Foundation for Cancer Research (protocol code: 2018-1177; date of approval: December 21, 2018).

Conflicts of Interest and Source of Funding: K.I. was financially supported by JSPS KAKENHI (Grant numbers JP22H02930 and JP23K18246), the Takeda Science Foundation, the Mochida Memorial Foundation for Medical and Pharmaceutical Research, the Ichiro Kanehara Foundation, Suzuki Foundation for Urological Medicine, Foundation for Promotion of Cancer Research in Japan, and the Yakult Bio-Science Foundation. For the remaining authors, none were declared.

Correspondence: Kentaro Inamura, MD, PhD, Division of Pathology, The Cancer Institute, Japanese Foundation for Cancer Research 3-8-31 Ariake, Koto-ku, Tokyo 135-8550, Japan (e-mail: kentaro.inamura@jfcr.or.jp)

Supplemental Digital Content is available for this article. Direct URL citations are provided in the HTML and PDF versions of this article on the journal's website, www.ajsp.com.

Inverted urothelial papilloma (IUP) is a benign tumor that exhibits a low recurrence rate after complete surgical resection, which is in contrast to the high recurrence rate of urothelial carcinoma (UC).[1–5] IUP was first described in 1927 by Paschkis as "polypoid adenomas" and was subsequently assigned its current nomenclature in 1963 by Potts and Hirst.[6] IUP primarily develops in the neck and trigone regions of the bladder and is predominantly diagnosed in men, typically manifesting in men aged 50 to 60 years.[1–5] The tumor is characterized by an inverted downgrowth of the urothelium into the underlying stroma while maintaining the surface of morphologically normal urothelial cells.[1,7–13] IUP was initially classified by Kunze et al[2] into trabecular and glandular subtypes based on distinct clinicopathological features; however, the relationship between these subtypes and their respective mutational characteristics has not been elucidated yet.

Next-generation sequencing of IUPs was first conducted by McDaniel et al[14] in 2014; using a 50-gene panel, they identified *HRAS* mutations in 3 out of 5 IUP cases,[14] suggesting the potential involvement of RAS pathway activation in IUP pathogenesis. Similarly, Isharwal et al[15] conducted next-generation sequencing for 11 IUP cases

and identified recurrent mutations in *HRAS* or *KRAS*, while also demonstrating the absence of *FGFR3*-activating mutations in IUPs. On the contrary, a few previous studies have reported *FGFR3* mutations in IUPs,[14,16] rendering the *FGFR3* status in IUPs inconclusive. Owing to the limited number of molecularly characterized IUP cases,[5,14–23] the molecular features of IUP and their associations with various clinicopathological characteristics, such as trabecular and glandular subtypes, remain poorly understood.

To address these knowledge gaps, we investigated the mutational landscape, clinicopathological features, and genotype-phenotype associations of IUP in a cohort of 39 consecutive cases of IUP arising in the urinary bladder. This study represents the largest consecutive series of molecularly analyzed IUP cases to date. Furthermore, we conducted an immunohistochemical analysis of the RAS Q61R mutation to visualize the neoplastic nature of the morphologically normal overlying urothelial cells, which has been a long-standing enigma in urologic pathology.

PATIENTS AND METHODS

Tissue Samples and Patient Data

We retrospectively analyzed tissue samples and patient data obtained from a consecutive cohort of 39 Japanese patients diagnosed with IUP of the urinary bladder, after transurethral tumor resection, at The Cancer Institute Hospital of Japanese Foundation for Cancer Research, Tokyo, Japan, between January 12, 2006 and September 22, 2022. The clinical data, including age, sex, history of smoking, tumor location, medical history, and follow-up data, were collected by reviewing the patient's medical records. The study protocol was approved by the Institutional Review Board of the Japanese Foundation for Cancer Research (approval number: 2018-1177). The requirement for informed consent was waived because of the retrospective nature of this study. The resected tissue samples were collected and handled in accordance with standard protocols for pathologic examination and diagnosis.

Pathologic Evaluation

For the pathologic assessment of the study specimens, 2 pathologists (K.K. and K.I.) independently reviewed hematoxylin and eosin–stained 4 μm thick sections of formalin-fixed paraffin-embedded (FFPE) specimens obtained from the patients with IUP. In cases where the 2 pathologists disagreed on the interpretation of the samples, a consensus was reached through discussion and joint review of the specimens. Cases that did not reach a consensus were excluded from this study. The diagnosis of IUP was made based on the criteria described in the fifth edition of the World Health Organization Classification of the Urinary and Male Tumors.[7] Using hematoxylin and eosin–stained sections, we examined each tumor for the presence of the following specific morphologic features: palisading pattern (a single layer of relatively long cells arranged parallel to one another), streaming pattern (an intermingled structure of centrally anastomosing urothelial cords), cystic changes (characterized by a luminal structure often filled with colloidal material), papillary architecture (manifesting as an exophytic papillary structure), and foamy vacuolated cytoplasm (relatively large and clear vacuoles in the cytoplasm).[24]

Immunohistochemical Analysis

Immunohistochemical analysis was conducted on 4 μm-thick FFPE sections using an anti-RAS Q61R rabbit monoclonal antibody (ab227658; clone: SP174; diluted 1:100; Abcam), which is known to have specificity for the detection of Q61R mutations in RAS family genes.[25] Immunostaining was conducted using the Leica Bond III automated staining system (Leica Microsystems, Buffalo Grove) with an incubation period of 60 minutes at 100 °C and pH 9.

Molecular Analysis

Targeted sequencing of 340 tumor-associated genes, including the *TERT* promoter region (Supplemental Table 1, Supplemental Digital Content 1, http://links.lww.com/PAS/B736, which lists the 340 genes used) was performed. DNA extraction was performed using macrodissections of 10 μm thick FFPE sections, with the number of sections ranging from 5 to 10 depending on tumor size. DNA was isolated using the AllPrep DNA/RNA FFPE kit (Qiagen) according to the manufacturer's instructions. The quantity and quality of the DNA were determined using a fluorescent DNA-binding dye and agarose gel electrophoresis, respectively. To obtain information on tumor-associated genes, we designed a customized panel of 340 target genes, including the *TERT* promoter region (Supplemental Table 1, Supplemental Digital Content 1, http://links.lww.com/PAS/B736, which lists the 340 genes used), using SureDesign, a web-based tool (https://earray.chem.agilent.com/suredesign/). To generate standard exome capture libraries, we used the Agilent SureSelect Target Enrichment protocol for the Illumina paired-end sequencing library (version C2, December 2018), together with an input of 200 ng FFPE DNA. The SureSelect Custom Tier2 (design ID: 3424131) probe set was used in all cases. The captured DNA was sequenced using the HiSeq X platform (Illumina).

Statistical Analyses

All statistical analyses were conducted using EZR software version 1.61 (Saitama Medical Center).[26] Categorical variables were compared between groups using the Fisher exact test, whereas continuous variables were compared using the paired *t* test. All statistical tests were 2-sided, and statistical significance was defined at $P < 0.05$.

RESULTS

Clinical Features

The mean patient age at diagnosis was 61.1 years (range: 40 to 76 y; SD: 10.2). The patients were predominantly male, with a male-to-female ratio of 8.8:1.

Two-thirds of the patients (27 cases) had a history of smoking (Fig. 1). The tumors were predominantly located at the neck (24 cases), followed by the trigone (9 cases), lateral wall (4 cases), and posterior wall (2 cases) of the bladder. None of the patients had a history of IUP or UC. No recurrence or carcinoma development was observed during the follow-up period (median: 13.1 mo; range: 0.23 to 190 mo).

Morphologic Findings

In all cases, the tumor exhibited an inverted downgrowth pattern from the morphologically normal overlying urothelium, with anastomosing cords or small regular nests. Mitotic figures were rare and limited to the basal layer. The most common morphologic feature observed was the palisading pattern (95%), followed by foamy vacuolated cytoplasm (67%), streaming pattern (64%), papillary architecture (56%), and cystic changes (51%; Fig. 1). Representative images are shown in Figure 2.

Driver mutations in RAS Family Genes

Targeted capture sequencing of 340 tumor-associated genes identified recurrent driver mutations in RAS family genes (*HRAS*, *KRAS*, and *NRAS*) in 87% (34/39) of cases (Supplemental Table 2, Supplemental Digital Content 2, http://links.lww.com/PAS/B737, which summarizes pathogenic mutations in the 39 IUP cases). Of these, 72% (28/39) were *HRAS* mutations, mostly with Q61R (15 cases), followed by Q61K (11 cases) and Q13R (2 cases), as depicted in Figure 1. In addition, *KRAS* mutations were detected in 5 cases (13%), comprising G12V (3 cases) and G12R (2 cases). Furthermore, *NRAS* Q61R mutation was detected in 1 case. The remaining 5 cases lacked either *HRAS*, *KRAS*, or *NRAS* mutations.

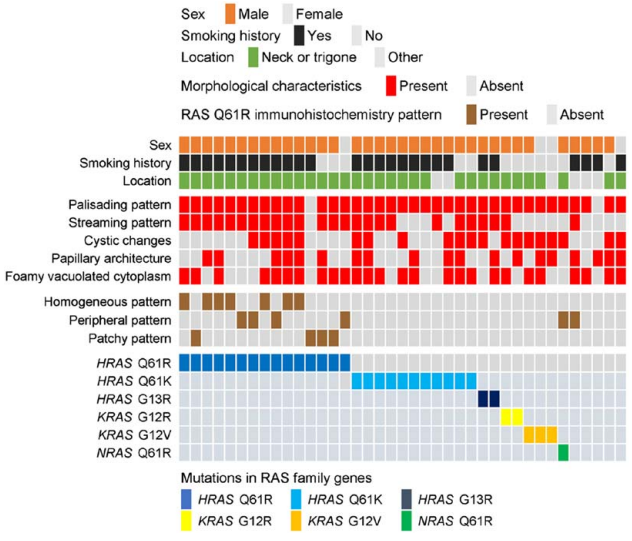

FIGURE 1. Clinicopathological features and mutations in RAS family genes of IUP.

Other Mutations

Mutations commonly observed in UC, such as those in *FGFR3*, *TP53*, *PIK3CA*, *CDKN1A*, *ARID1A*, *KDM6A*, *KMT2D*, *KMT2C*, *KMT2A*, *RB1*, *STAG2*, *CREBBP*, *TSC1*, and the *TERT* promoter regions, were not observed in any of the 39 IUP cases (Supplemental Table 2, Supplemental Digital Content 2, http://links.lww.com/PAS/B737, which summarizes pathogenic mutations in the 39 IUP cases).

Relationships Between *HRAS*/*KRAS* Mutations and Clinicopathological Characteristics

We found significant associations between the presence of RAS family gene mutations and clinicopathological features (Table 1). Specifically, *HRAS* mutations were significantly associated with a history of smoking ($P = 0.017$), localization to the bladder neck or trigone ($P = 0.042$), and streaming pattern in morphology ($P < 0.001$). In contrast, *KRAS* mutations were associated with the absence of streaming pattern ($P = 0.047$) and the presence of cystic changes ($P = 0.005$) in morphology, and all 5 *KRAS*-mutated IUPs developed in never-smoking individuals ($P = 0.001$).

RAS Q61R Immunohistochemistry

Among the 39 IUP cases, 17 showed diffuse staining in RAS Q61R immunohistochemistry with granular cytoplasmic and membranous patterns, whereas 22 cases did not display any staining.

Of the 17 RAS Q61R-immunopositive IUP cases, 15 had the *HRAS* Q61R mutation, 1 had the *NRAS* Q61R mutation, and 1 had no RAS mutation, demonstrating 94% specificity for Q61R mutations in RAS family genes. Furthermore, all cases with Q61R mutations were positive for RAS Q61R immunohistochemistry, indicating 100% sensitivity.

RAS Q61R immunohistochemistry of the morphologically normal overlying urothelial cells showed positive staining in all 16 cases with the Q61R mutation, albeit to varying degrees. Three distinct staining patterns were observed: homogeneous (54%, 7 cases), peripheral (31%, 5 cases), and patchy (25%, 4 cases; Fig. 1). In the homogeneous pattern (Fig. 3A, D), all the overlying urothelial cells were uniformly stained and considered neoplastic. In the peripheral pattern (Fig. 3B, E), the overlying urothelial cells were peripherally and continuously stained, indicating the neoplastic nature of the peripheral overlying cells. In the patchy staining pattern (Fig. 3C, F), stained cells were distributed in patches over the surface, and the spread of the neoplastic cells was considered pseudoinfiltrative in nature.

DISCUSSION

In this study, we investigated the mutational landscape, clinicopathological features, and genotype-phenotype associations of IUP arising in the bladder. Despite its morphologic resemblance to UC, IUP exhibited distinct molecular features, including recurrent mutations in RAS family genes and the absence of mutations that are commonly observed in UC. Notably, associations between RAS family gene

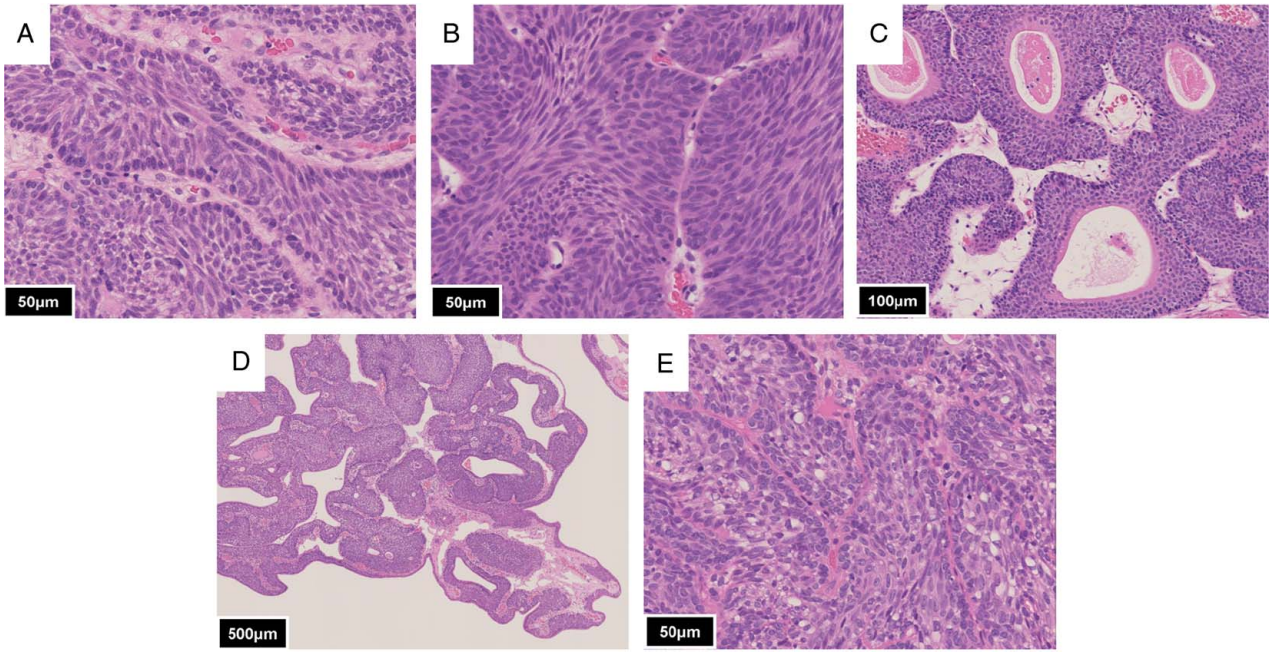

FIGURE 2. Morphological features of IUP. (A) Palisading pattern, (B) streaming pattern, (C) cystic changes, (D) papillary architecture, and (E) foamy vacuolated cytoplasm.

TABLE 1. Relationship Between *HRAS*/*KRAS* Mutations and Clinicopathological Characteristics of Patients With IUP

	***HRAS* mutations**			***KRAS* mutations**		
Variables	**Present; *N* = 28 (72%)**	**Absent; *N* = 11 (28%)**	***P***	**Present; *N* = 5 (13%)**	**Absent; *N* = 34 (87%)**	***P***
Age ((y); mean ± SD)	—	—	1.00	—	—	1.00
	61.1 ± 9.7	61.1 ± 11.5	—	58.8 ± 10.7	61.5 ± 10.1	—
Sex	—	—	0.060	—	—	0.072
Male	27 (96)	8 (73)	—	3 (60)	32 (94)	—
Female	1 (4)	3 (27)	—	2 (40)	2 (6)	—
Smoking history	—	—	0.017	—	—	0.001
Yes	23 (82)	4 (36)	—	0	27 (79)	—
No	5 (18)	7 (64)	—	5 (100)	7 (21)	—
Tumor location	—	—	0.042	—	—	1.00
Neck or trigone	26 (93)	7 (64)	—	4 (80)	29 (85)	—
Other	2 (7)	4 (36)	—	1 (20)	5 (15)	—
Palisading pattern	—	—	0.49	—	—	1.00
Present	27 (96)	10 (91)	—	5 (100)	33 (94)	—
Absent	1 (4)	1 (9)	—	0	2 (6)	—
Streaming pattern	—	—	<0.001	—	—	0.047
Present	23 (82)	2 (18)	—	1 (20)	24 (71)	—
Absent	5 (18)	9 (82)	—	4 (80)	10 (29)	—
Cystic changes	—	—	0.16	—	—	0.005
Present	12 (43)	8 (73)	—	5 (100)	15 (44)	—
Absent	16 (57)	3 (27)	—	0	19 (56)	—
Papillary architecture	—	—	0.30	—	—	0.66
Present	12 (43)	7 (64)	—	3 (60)	16 (47)	—
Absent	16 (57)	4 (36)	—	2 (40)	18 (53)	—
Foamy vacuolated cytoplasm	—	—	1.00	—	—	1.00
Present	19 (68)	7 (64)	—	3 (60)	23 (68)	—
Absent	9 (32)	4 (36)	—	2 (40)	11 (32)	—

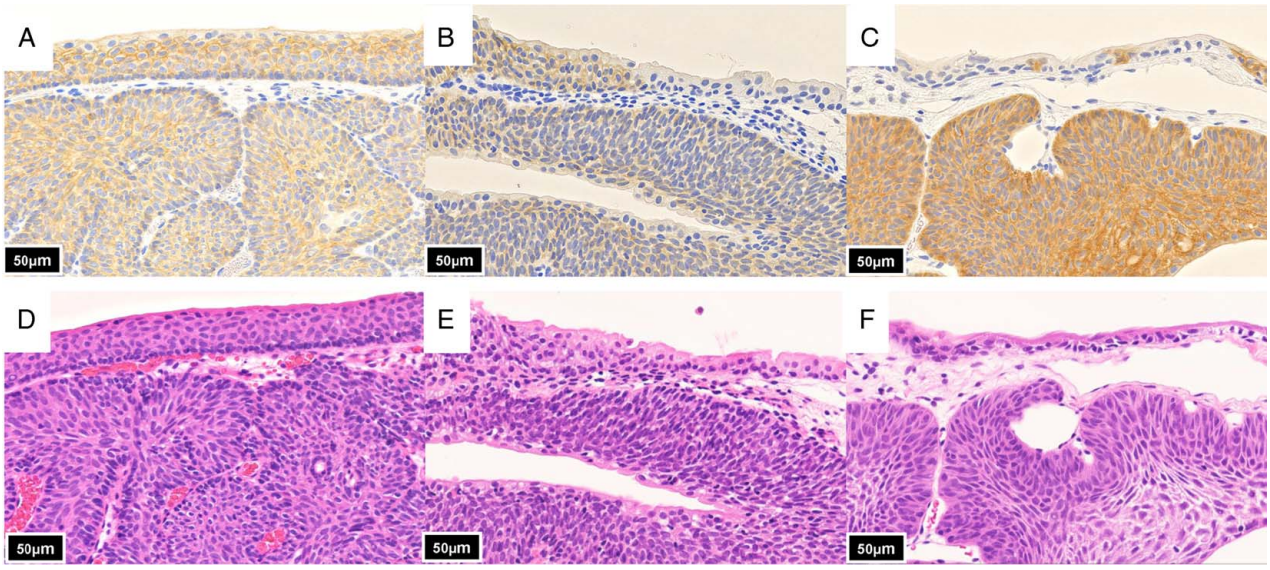

FIGURE 3. Staining patterns of morphologically normal overlying urothelial cells in (A–C) sections investigated using RAS Q61R immunohistochemistry, and (D–F) sections stained with hematoxylin and eosin. A and D, Homogeneous pattern. B and E, Peripheral pattern. C and F, Patchy pattern.

mutations and clinicopathological features were identified. Further investigations visually revealed the neoplastic nature of the overlying urothelial cells.

In this study, which represents the largest consecutive series of IUP cases analyzed to date, we conducted targeted sequencing of 340 tumor-associated genes to investigate its mutational landscape. Most IUP cases harbored a driver mutation in RAS family genes, with the *HRAS* Q61R mutation being the most prevalent; these results corroborate the findings of previous studies that also detected *HRAS* or *KRAS* mutations in IUPs.[14,15] We further determined the frequency of these mutations and identified *NRAS* in addition to *HRAS* and *KRAS* mutations in IUPs. In previous studies,[14,16] *FGFR3* mutations were observed in a subset of IUP cases, specifically in 1 of 5 cases studied by McDaniel et al[14] and 9 of 20 cases, including silent mutations, investigated by Lott et al.[16] Among these, only one *FGFR3*-mutated IUP case was illustrated, which displayed the typical characteristics of IUP but also posed a diagnostic challenge owing to its similarities with UC with an inverted growth pattern. In contrast, our examination of 39 IUP cases indicated the absence of mutations commonly observed in UC, including those of *FGFR3,* as well as *TP53*, *PIK3CA*, and the *TERT* promoter.[27–30] A driver mutation in RAS family genes, which regulate cell proliferation, differentiation, and survival, potentially promotes cancer development, especially when coupled with additional oncogenic mutations.[31] Our results suggested that a mutation of RAS family genes alone is insufficient for the malignant transformation of IUP. This may be because of oncogene-induced senescence (OIS), which is a cellular response to oncogenic stress that induces persistent cell-cycle arrest, thereby inhibiting the proliferation of cells harboring oncogenic mutations.[32–34] In IUP, OIS may prevent uncontrolled growth arising from a mutation in RAS family genes in the context of activated tumor suppressor genes such as *TP53*.[32–34] Although a small proportion of UC tumors also harbor driver mutations in RAS family genes, these are usually accompanied by additional oncogenic mutations such as *TP53* mutations. These concurrent mutations would counteract OIS, thus potentially driving malignancy.[27–29,32–34] Collectively, our analysis highlights the significance of RAS family gene mutations in IUP development, while emphasizing the mutational distinctions between IUP and UC.

We confirmed clinicopathological features of IUP, such as a male predominance, a history of smoking, and tumor localization to the bladder neck or trigone.[1–5] During the follow-up period, no recurrence or carcinoma development was observed in any IUP case, highlighting the clear distinction of the clinical course between IUP and UC. These data, along with those from earlier studies,[1–5,15] suggest that IUP can be sufficiently treated by complete transurethral resection without stringent surveillance protocols required for UC, highlighting the importance of correctly distinguishing between these entities for clinical management.

Our investigation revealed notable associations between RAS family gene mutations and the IUP subtypes. Specifically, our data suggested that *HRAS*-mutated and *KRAS*-mutated IUPs may correspond to trabecular and glandular subtypes, respectively. Trabecular-type IUPs show a streaming morphology and resemble IUPs induced in a rat model by N-butyl-N-nitrosamine, a compound found in cigarette smoke.[2,35] *HRAS*-mutated IUPs, associated with a smoking history and a streaming morphology in our data set, are likely of the trabecular type. In contrast, all *KRAS*-mutated IUPs developed in never-smoking patients and showed cystic changes in their

morphology, a characteristic commonly observed in glandular-type IUPs.[2] These observations suggested distinct mechanisms driving *KRAS*-mutated and *HRAS*-mutated IUPs, leading to the generation of different clinicopathological subtypes. These genotype-phenotype associations offer valuable insights into the interplay between molecular alterations and clinicopathological features in IUP pathogenesis.

The neoplastic nature of the overlying morphologically normal urothelial cells in IUP has thus far remained unclear. Through the application of RAS Q61R immunohistochemistry, we were able to visualize the neoplastic cells and discern their spread patterns. Staining patterns revealed 3 spread patterns of IUP neoplastic cells within the urothelial surface. The homogeneous pattern suggested that the entire overlying urothelial cell population was neoplastic. The peripheral pattern indicated that IUP neoplastic cells displaced contiguous sections of the overlying urothelial cells. In contrast, the patchy pattern suggested a pseudoinfiltrative spread of neoplastic cells within the surface urothelium. Further studies are needed to understand the mechanisms underlying the spread patterns within the IUP surface and their clinical implications.

Several limitations of this study should be acknowledged. First, we focused exclusively on IUP cases without including UC cases or directly comparing IUP and UC cases. Thus, our understanding of the distinct molecular characteristics of IUP and their potential association with UC remains limited. Second, although no IUP recurrence or carcinoma development was observed in any IUP case during the follow-up period, longer follow-up periods are needed to thoroughly assess the long-term outcomes and malignant potential of IUP. Third, although this is the largest sample analysis on IUP mutation signatures to date, the sample size of 39 patients is not sufficient to capture the entire clinical and molecular spectrum of IUP, necessitating even larger studies to validate our findings. Fourth, our single-institution study could have introduced a selection bias and limited the generalizability of our findings. Finally, the functional implications of the identified mutations warrant further investigation.

CONCLUSION

This study provides significant insights into the molecular and clinicopathological characteristics of IUP. By confirming recurrent driver mutations in RAS family genes, including *HRAS*, *KRAS*, and *NRAS*, as well as the absence of mutations commonly observed in UC, our findings demonstrated the characteristic mutational landscape of IUP, highlighting the importance of RAS pathway activation in its pathogenesis. Notably, we revealed the genotype-phenotype associations, suggesting that *HRAS*-mutated IUPs and *KRAS*-mutated IUPs correspond to trabecular and glandular subtypes, respectively. Moreover, using RAS Q61R immunohistochemistry, we visually demonstrated the neoplastic nature of the overlying morphologically normal urothelial cells and their spread patterns. Further research is warranted to validate our findings and translate them into diagnostic and therapeutic strategies for IUP.

ACKNOWLEDGMENTS

The authors thank Motoyoshi Iwakoshi, Keiko Shiozawa, Shuhei Ishii, and Miyuki Kogure for their technical assistance and Yuki Takano for her secretarial expertise.

REFERENCES

1. Sung MT, Maclennan GT, Lopez-Beltran A, et al. Natural history of urothelial inverted papilloma. *Cancer*. 2006;107:2622–2627.
2. Kunze E, Schauer A, Schmitt M. Histology and histogenesis of two different types of inverted urothelial papillomas. *Cancer*. 1983;51:348–358.
3. Witjes JA, van Balken MR, van de Kaa CA. The prognostic value of a primary inverted papilloma of the urinary tract. *J Urol*. 1997;158:1500–1505.
4. Picozzi S, Casellato S, Bozzini G, et al. Inverted papilloma of the bladder: a review and an analysis of the recent literature of 365 patients. *Urol Oncol*. 2013;31:1584–1590.
5. Eiber M, van Oers JM, Zwarthoff EC, et al. Low frequency of molecular changes and tumor recurrence in inverted papillomas of the urinary tract. *Am J Surg Pathol*. 2007;31:938–946.
6. Potts IF, Hirst E. Inverted papilloma of the bladder. *J Urol*. 1963;90:175–179.
7. Raspollini MR, Cho YM, He HY, et al. Inverted Urothelial Papilloma. In: Compérat EM, Netto GJ, Tsuzuki T, editors. *Urinary and male genital tumours*. 5th ed. Lyon (France): International Agency for Research on Cancer; 2022:136–137.
8. Bang H, Park H, Park S, et al. Clinicopathologic study of 60 cases of urothelial neoplasms with inverted growth patterns: reclassification by international consultation on urologic disease (ICUD) recommendations. *Ann Diagn Pathol*. 2020;44:151433.
9. Patel P, Reikie BA, Maxwell JP, et al. Long-term clinical outcome of inverted urothelial papilloma including cases with focal papillary pattern: is continuous surveillance necessary? *Urology*. 2013;82:857–860.
10. Amin MB, Gómez JA, Young RH. Urothelial transitional cell carcinoma with endophytic growth patterns: a discussion of patterns of invasion and problems associated with assessment of invasion in 18 cases. *Am J Surg Pathol*. 1997;21:1057–1068.
11. Sun JJ, Wu Y, Lu YM, et al. Immunohistochemistry and fluorescence in situ hybridization can inform the differential diagnosis of low-grade noninvasive urothelial carcinoma with an inverted growth pattern and inverted urothelial papilloma. *PLoS One*. 2015;10:e0133530.
12. Hodges KB, Lopez-Beltran A, Maclennan GT, et al. Urothelial lesions with inverted growth patterns: histogenesis, molecular genetic findings, differential diagnosis and clinical management. *BJU Int*. 2011;107:532–537.
13. Manini C, Angulo JC, López JI. Mimickers of urothelial carcinoma and the approach to differential diagnosis. *Clin Pract*. 2021;11:110–123.
14. McDaniel AS, Zhai Y, Cho KR, et al. HRAS mutations are frequent in inverted urothelial neoplasms. *Hum Pathol*. 2014;45:1957–1965.
15. Isharwal S, Hu W, Sarungbam J, et al. Genomic landscape of inverted urothelial papilloma and urothelial papilloma of the bladder. *J Pathol*. 2019;248:260–265.
16. Lott S, Wang M, Zhang S, et al. FGFR3 and TP53 mutation analysis in inverted urothelial papilloma: incidence and etiological considerations. *Mod Pathol*. 2009;22:627–632.
17. Akgul M, MacLennan GT, Cheng L. Distinct mutational landscape of inverted urothelial papilloma. *J Pathol*. 2019;249:3–5.
18. Almassi N, Pietzak EJ, Sarungbam J, et al. Inverted urothelial papilloma and urothelial carcinoma with inverted growth are histologically and molecularly distinct entities. *J Pathol*. 2020;250:464–465.
19. Wang CC, Huang CY, Jhuang YL, et al. Biological significance of TERT promoter mutation in papillary urothelial neoplasm of low malignant potential. *Histopathology*. 2018;72:795–803.

20. Cheng L, Davidson DD, Wang M, et al. Telomerase reverse transcriptase (TERT) promoter mutation analysis of benign, malignant, and reactive urothelial lesions reveals a subpopulation of inverted papilloma with immortalizing genetic change. *Histopathology*. 2016;69:107–113.
21. Sung MT, Eble JN, Wang M, et al. Inverted papilloma of the urinary bladder: a molecular genetic appraisal. *Mod Pathol*. 2006;19:1289–1294.
22. Williamson SR, Zhang S, Lopez-Beltran A, et al. Telomere shortening distinguishes inverted urothelial neoplasms. *Histopathology*. 2013;62:595–601.
23. Jung M, Lee C, Han D, et al. Proteomic-based machine learning analysis reveals PYGB as a novel immunohistochemical biomarker to distinguish inverted urothelial papilloma from low-grade papillary urothelial carcinoma with inverted growth. *Front Oncol*. 2022;12:841398.
24. Fine SW, Epstein JI. Inverted urothelial papillomas with foamy or vacuolated cytoplasm. *Hum Pathol*. 2006;37:1577–1582.
25. Nakaguro M, Tanigawa M, Hirai H, et al. The diagnostic utility of RAS Q61R mutation-specific immunohistochemistry in epithelial-myoepithelial carcinoma. *Am J Surg Pathol*. 2021;45:885–894.
26. Kanda Y. Investigation of the freely available easy-to-use software 'EZR' for medical statistics. *Bone Marrow Transplant*. 2013;48:452–458.
27. Pietzak EJ, Bagrodia A, Cha EK, et al. Next-generation sequencing of nonmuscle invasive bladder cancer reveals potential biomarkers and rational therapeutic targets. *Eur Urol*. 2017;72:952–959.
28. Robertson AG, Kim J, Al-Ahmadie H, et al. Comprehensive molecular characterization of muscle-invasive bladder cancer. *Cell*. 2017;171:540–556.e525.
29. Knowles MA, Hurst CD. Molecular biology of bladder cancer: new insights into pathogenesis and clinical diversity. *Nat Rev Cancer*. 2015;15:25–41.
30. Inamura K. Bladder cancer: new insights into its molecular pathology. *Cancers (Basel)*. 2018;10:100.
31. Malumbres M, Barbacid M. RAS oncogenes: the first 30 years. *Nat Rev Cancer*. 2003;3:459–465.
32. Minoo P, Jass JR. Senescence and serration: a new twist to an old tale. *J Pathol*. 2006;210:137–140.
33. Collado M, Serrano M. Senescence in tumours: evidence from mice and humans. *Nat Rev Cancer*. 2010;10:51–57.
34. Schmitt CA, Wang B, Demaria M. Senescence and cancer—role and therapeutic opportunities. *Nat Rev Clin Oncol*. 2022;19:619–636.
35. Kunze E. Development of urinary bladder cancer in the rat. *Curr Top Pathol*. 1979;67:145–232.